BIOCHEMICAL AND BIOPHYSICAL RESEARCH COMMUNICATIONS **242,** 158–163 (1998)
ARTICLE NO. RC977875

Three-Dimensional Molecular Modeling Explains Why Catalytic Function for Angiotensin-I Is Different between Human and Rat Chymases

Daisuke Yamamoto,* Naotaka Shiota,† Shinji Takai,† Toshimasa Ishida,‡ Hideki Okunishi,§ and Mizuo Miyazaki†,[1]

**Medical Computation Center and †Department of Pharmacology, Osaka Medical College, Takatsuki, Osaka 569, Japan; ‡Department of Physical Chemistry, Osaka University of Pharmaceutical Science, Takatsuki, Osaka 569, Japan; and §Department of Pharmacology, Shimane Medical University, Izumo, Shimane 693, Japan*

Received November 12, 1997

Although angiotensin (ANG)-I is a substrate sensitive to chymase, the cleavage site differs among the chymase families. While human chymase (HC) hydrolyses the Phe8-His9 bond of ANG-I to ANG-II, rat chymase (RMCP-I) degrades the Tyr4-Ile5 bond of ANG-I to the inactive fragments. To clarify this different catalysis for ANG-I at the atomic level, three-dimensional structures of HC and RMCP-I were constructed by the molecular dynamic simulation. The energy-refined models clearly showed the significant difference in the electrostatic potential of the solvent surface. From the modeling study of their complex structures with ANG-I, the functional difference between both enzymes was clearly related with the electrostatic difference, especially at the C-terminal substrate-binding site. © 1998 Academic Press

Angiotensin (ANG)-II plays diverse biological function in the development of cardiovascular diseases. It is well known that the ANG-II is produced in blood circulation through the renin-angiotensin system (RAS) [1]. However, it has been recently demonstrated by the molecular biological study that the ANG-II is locally biosynthesized to regulate cell function and tissue reorganization in paracrine manner [2]. Our previous studies showed that the chymase also contributes to the generation of ANG-II in blood vessels of human, monkey, and dog [3-6]. The chymase belongs to a chymotrypsin-like serine protease family. It is characteristic that the catalytic efficiency and product of the chymase markedly differs among the different species, although their amino acid sequences are highly homologous to one another. Although ANG-I (Asp1-Arg2-Val3-Tyr4-Ile5-His6-Pro7-Phe8-His9-Leu10) is a substrate of the chymase, the cleavage site is different among the chymase family. Human chymase (HC) cleaves the Phe8-His9 bond of ANG-I to generate ANG-II specifically [7], while rat chymase known as rat mast cell protease I (RMCP-I) cleaves the Tyr4-Ile5 bond and consequently degrades the ANG-I to biologically inactive fragments [8]. It appears important to elucidate the structural basis concerning such a species difference of the enzymatic activity at the atomic level, because this is surely useful to effectively design the inhibitor which can control the function of chymase. On the other hand, the molecular dynamics (MD) simulation [9, 10] has been developed as a convenient and confirmed methodology in the field of the structural biochemistry, supported by the acute development of computational facilities and the accumulation of three-dimensional (3D) atomic coordinates of biomolecules. Its application includes the 3D prediction of an unknown biomolecule from the homologous 3D structure [11] and the quantitative estimation of conformation-activity relationship between the mutated proteins [12].

Concerning the 3D structure of chymase, the X-ray structure of rat mast cell protease II (RMCP-II) is now available [13]. To make clear the structural/functional difference between the ANG-I-binding pockets in HC and RMCP-I at the atomic level, we report here the prediction of 3D structures of HC and RMCP-I and their complexes with ANG-I using the X-ray atomic coordinates of RMCP-II and the MD simulation.

MATERIALS AND METHODS

Molecular modeling of HC and RMCP-I 3D structures from X-ray structure of RMCP-II. An alignment between chymases of different

[1] Corresponding Author. Fax: +81-726-84-6518.

0006-291X/98 $25.00

```
           1                   20          _          40     +_             60
HC         IIGGTESKPH SRPYMAYLEI  VTSNGPSKFC GGFLIRRNFV  LTAAHCAGRS ITVTLGAHNI
RMCP-I     IIGGVESRPH SRPYMAHLEI  TTERGYKATC GGFLVTRQFV  MTAAHCKGRE TTVTLGVHDV
id2        **** **.** ****** ***   *  *    * ****. *.**  .***** **   ***** *..
RMCP-II    IIGGVESIPH SRPYMAHLDI  VTEKGLRVIC GGFLISRQFV  LTAAHCKGRE ITVILGAHDV
id3        **** ** ** ****** *.*   *  *    * ****. *.**  .***** **   ** ** *..
          61                  80         +          100                  120
HC         TEEEDTWQKL EVIKQFRHPK  YNTSTLHHDI MLLKLKEKAS  LTLAVGTLPF PSQFNFVPPG
RMCP-I     SKTESTQQKI KVEKQIVHPN  YNFYSNLHDI MLLKLQKKAK  VTPAVDVIPL PQPSDFLKPG
id2        .  * * **.  * **. **.  **  .  *** *****. **   .* **. .*. *   .*. **
RMCP-II    RKRESTQQKI KVEKQIIHES  YNSVPNLHDI MLLKLEKKVE  LTPAVNVVPL PSPSDFIHPG
id3           * * **.  * **. *    **     *** *****  *    .* **  .*. *   .*. **
         121 _                 140              _     160      _              180
HC         RMCRVAGWGR TGVLKPGSDT  LQEVKLRLMD PQACSHFRDF  DHNLQLCVGN PRKTKSAFKG
RMCP-I     KMCRAAGWGQ TGVTKPTSNT  LREVKQRIMD KEACKNYFHY  NYNFQVCVGS PRKIRSAYKG
id2        .*** ****. *** ** *.*  *.*** *.**  .** .. ..  . *.*.***. *** .**.**
RMCP-II    AMCWAAGWGK TGVRDPTSYT  LREVELRIMD EKACVDYRYY  EYKFQVCVGS PTTLRAAFMG
id3         **. ****. ***  * * *  *.**  *.**   ** ..  .  . ..*.***. *   ..*. *
         181+     _            200                 220
HC         DSGGPLLCAG VAQGIVSYGR  SDAKPPAVFT RISHYRPWIN  QILQAN
RMCP-I     DSGGPLVCAG VAHGIVSYGR  GDAKPPAVFT RISPYVPWIN  KVIKGKD
id2        ******.*** **.*******  .********* *** * ****  .....
RMCP-II    DSGGPLLCAG VAHGIVSYGH  PDAKPPAIFT RVSTYVPTIN  AVIN
id3        ******.*** **.******.   ******.** *.* * * **  ..
```

FIG. 1. Alignment table of HC, RMCP-I, and RMCP-II. The lines of 'id2' and 'id3' show identical (*) and similar (.) residues between the HC and RMCP-I and among the HC, RMCP-I and -II, respectively. Homologous factor are as follows: HC - RMCP-I, identical 61%, similar 78%; HC - RMCP-I, identical 59%, similar 73%; RMCP-I - RMCP-II, identical 73%, similar 84%. Cysteine residues (_) forming disulfide bonds and the active triad (+) are commonly conserved in all chymases. The multiple alignment was dome using CLUSTAL-W version.1.6 program [14] in the following default condition, i.e., weight matrices of BLOSUM series [18], gap opening penalty =10.0, gap extension penalty =0.05, protein gap separation distance = 8 with residue specific penalties where hydrophilic residues = GPSNDQEKR. The definition of similar residues is summarized by M. Vingron et.al. [19].

species, analyzed by CLUSTAL-W program [14], is shown in Fig.1, where the serial number of amino acid residues of RMCP-II [13] is used for the HC and RMCP-I model buildings. The atomic coordinates (PDB code: 3RP2) of RMCP-II backbone chain were used for the constructions of the HC and RMCP-I 3D structures, and the atomic coordinates of respective side chains were arbitrary built using a graphical interactive system QUANTA (Molecular Simulation Inc., USA). The molecular dynamics (MD) simulation program CHARMm2.2 [10] was used for the conformational optimization. The standard residue topology file (RTF) was prepared in the iteration steps, in which the residue specifications of total charge, atom definitions, bond, angle, dihedral/improper angle, hydrogen-bond donor/acceptor, and internal atomic coordinate information for each residue are included, and these were used for the calculations of internal (bond, bond angle and torsion) and external (electrostatic and Van der Waals) energy terms for the minimization of total energy [10]. A coordinate set of RMCP-I was calculated by Remington S.J. *et al.* using their RMCP-II X-ray structure[13], but it was replaced only sidechain conformation fixing the backbone of RMCP-II molecule. For the consideration of the slight differences between backbone structure of chymases, the whole molecules were unfixed in a series of our optimization except for the preliminary steps.

2193 atoms for HC or 2169 atoms for RMCP-I were subjected into the 200 steps of energy minimization before the MD simulation, where solvent molecules were not included. Cutoff distance for non-bonded interactions was set to 15Å, and dielectric constant was 1.0 in the calculating of electrostatic energy. Non-bonded pair list was updated every 25 steps. To avoid the conformational dependency of the initial energy-minimized structure, 10ps MD simulation was performed, where 1004 (HC) and 1054 (RMCP-I) TIP3 water molecules [15] existing within 8Å from the molecular surfaces of respective enzymes were included. The calculation condition is as follows: iteration step=0.002ps, 300 steps of heat-up and equilibrium, 5000 steps of molecular simulation, no constraint for protein atoms. The most stable model in the final 2000 steps was then subjected to the energy minimization. The final structures of HC and RMCP-I enzymes consist of 5181 and 5370, atoms and have total energies of -1.96×10^5 and -2.09×10^5 kcal/mol and r.m.s. forces of 0.495 and 0.465 kcal/molÅ, respectively.

Molecular modelings of HC - and RMCP-I - ANG-I complexes. Atomic coordinates of ANG-I were generated as a beta-strand structure using the sequence builder tool in QUANTA system and were relaxed with TIP3 water molecules within 8Å from each atom of ANG-I. The conformation of Pro7 was employed as *trans*. Taking into the consideration that the scission position of ANG-I is different depending on the species of chymase (Tyr4-Ile5 for HC and Phe8-His9 for RMCP-I), two kinds of binding modes were adopted for the docking of ANG-I to respective enzymes, i.e., (i) the side chain of Tyr4 (for 4-5 cleavage model) or Phe8 (for 8-9 cleavage model) of ANG-I was placed at the entrance of the P1 holes and (ii) the remaining moiety of ANG-I was then fitted along the deep catalytic clefts of respective enzymes. During the preliminary optimization, no solvent molecules were included, and only residues within 8Å from ANG-I atoms were subjected to 200 steps energy minimization. Then 10ps MD simulation was performed for each model including TIP3 water molecules within 8Å from the surface atoms of each complex, where the condition is as follows: iteration step= 0.002ps, 300 steps of heat-up and equilibrium, 5000 steps of MD simulation, no constraint for protein atoms. In this calculation, no any constraint was imposed on the atomic pairs between ANG-I and chymase. The most stable model in the iterations of the final 2000 steps was sub-

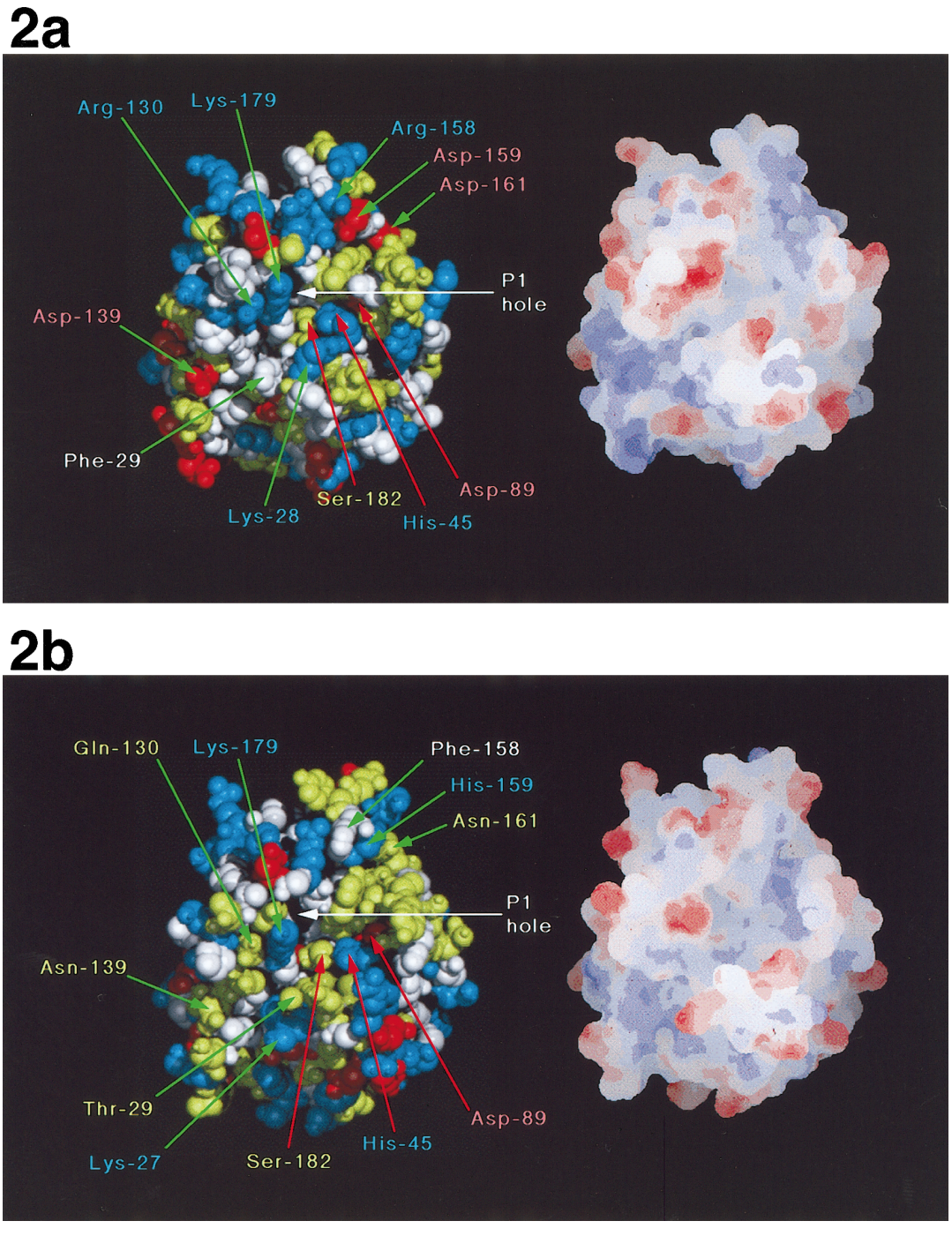

FIG. 2. Exposed residues and electrostatic potentials of active clefts of HC and RMCP-I. Exposed residues and electrostatic potentials of the active clefts in HC (a) and RMCP-I (b) are displayed in the right and left sides respectively. The active center is indicated by red arrows. The positive, negative, non-charged hydrophilic, and hydrophobic residues are indicated by blue, red, yellow, and white spheres, respectively. The positive and negative charges on the molecular surface in the vacuous circumstance are colored with red and blue, respectively. Calculations of electrostatic potential were performed by QUANTA system using partial atomic charges obtained from CHARMm calculations [10] with a solvent probe radius of 1.4Å and a dot density of 15dots/Å^2. Maximum and minimum potential values on the enzyme were 54.78 and −44.2 kcal/mol in HC, and 78.0 and −45.9 kcal/mol in RMCP-I. For the purpose of comparing HC and RMCP-I, however, a range from −50.0 kcal/mol to 60.0 kcal/mol was figured.

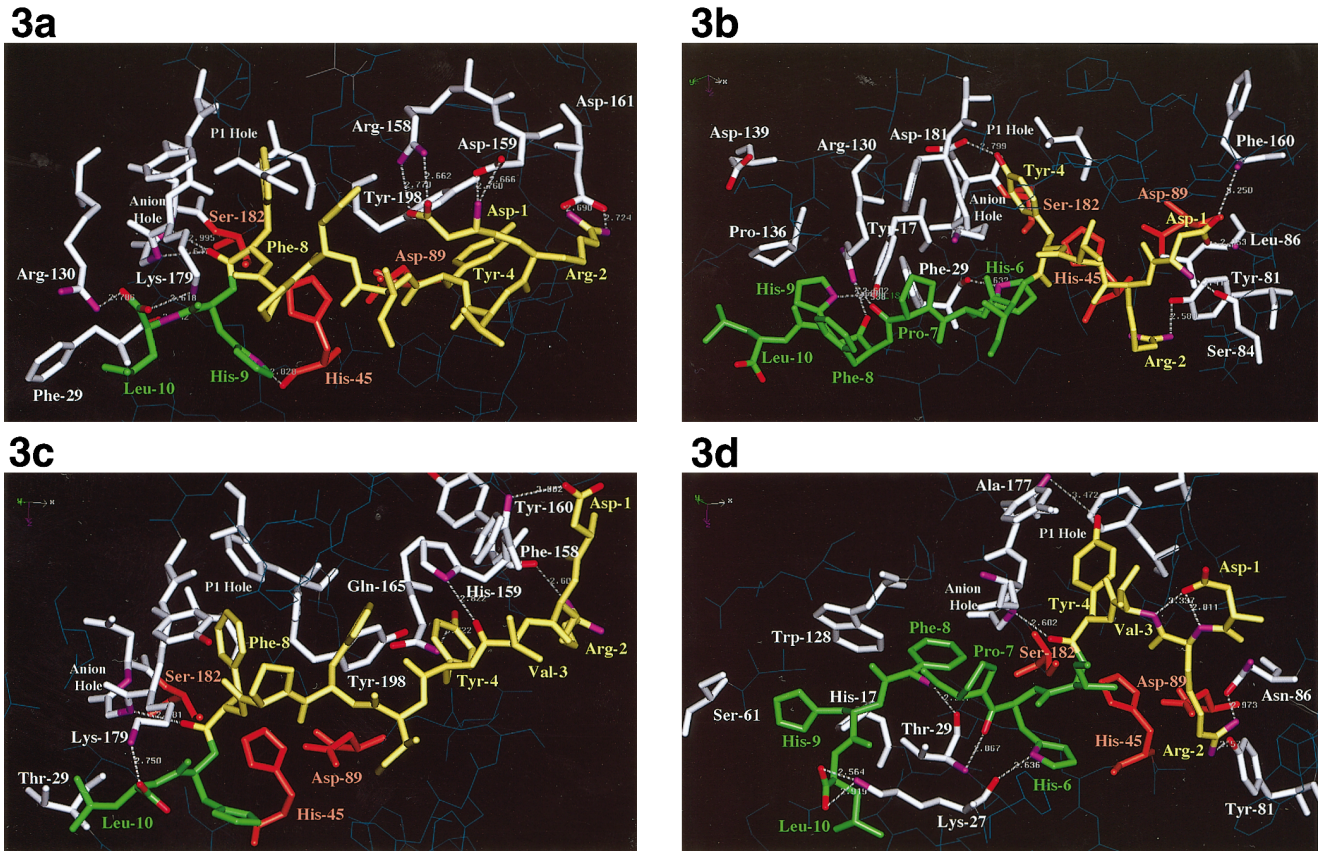

FIG. 3. Structures of the 8-9 and 4-5 cleavage models of HC - ANG-I and RMCP-I - ANG-I complexes. The structures of the 8-9 (a) and 4-5 (b) cleavage models of HC - ANG-I complex and the 8-9 (c) and 4-5 (d) cleavage models of RMCP-I - ANG-I complex are shown. Each active center, N-terminal and C-terminal sides of ANG-I, and the related residues are indicated by orange, yellow, green, and white colors, respectively. Nitrogen and oxygen atoms related to the electrostatic interactions and/or hydrogen bonds are marked with purple and red colors, respectively, together with their interatomic distances.

jected to the energy minimization. The final structures consist of 5347, 5356, 5380, and 5434 atoms, and have total energies of -2.05×10^5, -2.04×10^5, -2.05×10^5, and -2.10×10^5 kcal/mol and averaged root-mean-square (r.m.s) forces of 0.455, 0.490, 0.492, and 0.448 kcal/molÅ for HC, 8-9 cleavage model, HC, 4-5 cleavage model, RMCP-I, 8-9 cleavage model, and RMCP-I, 4-5 cleavage model, respectively. All of the calculations and graphical operations were carried out on a IRIS Indigo2 workstation (Silicon Graphics Inc., USA).

RESULTS AND DISCUSSION

The alignments among the HC, RMCP-I, and RMCP-II amino acid sequences are shown in Fig.1. These sequences are highly homologous. Six cysteine residues related to the disulfide bond formations in RMCP-II are all conserved in HC and RMCP-I, and Ser182, His45, and Asp89 constituting the active triad are also commonly conserved. No significant differences from the 3D structure of RMCP-II were observed for both HC and RMCP-I; the r.m.s difference was 1.04 and 1.09 Å for Cα carbon atoms, and 1.02 and 1.05 Å for main chain atoms of HC and RMCP-I, respectively. The active triad is located at the center of the cleft on the surface between two domains.

The electrostatic potential around the active site in HC and RMCP-I models is shown in Fig.2, together with the notation of exposed residues. The electrostatic potential at the active groove of RMCP-I seemed to be undulating more gently than that of HC. The Asp139 of HC, which is located at C-terminal side, shows more clear undulation of negative charge than that of RMCP-I, and the positive charges of Arg130 and Lys179 in HC are located close to the place so as to function synergistically. On the other hand, the charged residues of Arg158, Asp159, and Asp161 in HC, which correspond to those of Phe158, His159 and Asn161 in RMCP-I, respectively, are located at N-terminal side. As a result, the active site of HC is characteristically surrounded by the charged residues, while that of RMCP-I is constituted by the non-charged hydrophilic residues. Although the shape of cleft (active site) as a whole is similar to each other, that of HC is narrowed down by Phe29 side chain, compared with that of RMCP-I by

TABLE I

Intermolecular Interactions of A-I with HC or RMCP-I in Each Complex Model

	HC 8-9 model		HC 4-5 model		RMCP-I 8-9 model		RMCP-I 4-5 model	
	A-I	HC	A-I	HC	A-I	RMCP-I	A-I	RMCP-I
Hydrogen Bonds and Electrostatic Interactions[1)]	Asp1 N Asp1 N Asp1 OD1 Asp1 OD2 Arg2 NH1 Arg2 NH2 Leu10 OT1 Leu10 OT2	Asp159 OD1 Asp159 OD2 Arg158 NH1 Arg158 NH2 Asp161 OD1 Asp161 OD2 Lys179 NZ Arg130 NH1			Leu10 OT1 Leu10 OT2	Lys179 NZ Lys179 NZ	Leu10 OT1	Lys27 NZ
Hydrogen Bonds[1,2)]	*Phe8 O *Phe8 O His9 ND1	Gly180 N Asp181 N His-45 O	Asp1 N Asp1 OD1 Asp1 OD2 Arg2 NH1 Tyr4 OH His6 ND1 Pro7 O Phe8 O His9 ND1	Ser84 O Leu86 N Phe160 N Tyr81 OH Asp181 OD1 Phe29 O Arg130 NH1 Arg130 NH1 Tyr17 OH	Asp1 OD1 Arg2 NH1 Val3 O Tyr4 OH *Phe8 O	Tyr160 N Phe158 O His159 ND1 Gln165 NE2 Gly180 N	Arg2 NH1 Arg2 NH2 Tyr4 OH *Tyr4 O His6 ND1 His6 O Phe8 N	Asn86 OD1 Tyr81 OH Ala177 O Gly180 N Lys27 O Thr29 N Thr29 O
Hydrophobic Interactions[3)]	Tyr4 Leu10	Tyr198 Phe29	Pro7	Phe29			Phe8	Trp128

1) Hydrogen bonds and electrostatic interactions were listed with 3.6 Å of cutoff distance.

2) Interactions between the peptide moiety of A-I cleavage and the anion hole of each chymase were marked as *. HC 4-5 complex model has no intermolecular interaction related with the anion hole.

3) Hydrophobic interactions were listed where hydrophobic sidechains were closed in 4.0Å except for the interactions related with P1 hole.

Thr29. In addition, the lysine residue of Lys28 in HC and Lys27 in RMCP-I, both of which are located on the same β-sheet structure, are placed at inside and outside of the enzyme, respectively. These electric and steric differences at the active sites of HC and RMCP-I could be a main origin of exhibiting their diverse digestion and/or substrate-specificity for ANG-I (discussed later).

To investigate the different catalytic function of these chymases against ANG-I at the atomic level, two kinds of ANG-I binding modes (4-5 and 8-9 cleavage models) were considered for the complex formation with HC and RMCP-I. Respective final structures, obtained by the MD simulation, are shown in Fig.3. The intermolecular interactions between the ANG-I and enzyme in the respective complexes are summarized in Table I.

In the 8-9 cleavage models (Fig.3a and 3c), it is characteristic that both chymases hold the side chain of ANG-I Phe8 in the P-1 hole and the negative charge of ANG-I C-terminal is placed near at the side chain of Lys179. The ANG-I in HC complex is tightly stabilized by hydrogen bonds or electrostatic interactions of Arg130 - ANG-I C-terminal, Arg158 - ANG-I Asp1, Asp159 - ANG-I N-terminal, and Asp161 - ANG-I Arg2 (Fig.3a and Table I). On the other hand, the ANG-I complexed with RMCP-I is fixed to the active site *via* hydrogen bonds of Lys179 - ANG-I Leu10, and the cleavage peptide of Phe8 - His9 is closed to the anion hole, Gly-180 N (Fig.3c).

In the 4-5 cleavage model, on the other hand, many hydrogen bonds stabilized the whole structure of HC - ANG-I complex (Table I). However, the charge repulsion could be observed between the Asp139 of HC and ANG-I C-terminal carboxylate (Fig.3b) and consequently the 4-5 amide moiety of ANG-I is considerably far located from the active center of HC (ANG-I Tyr4 O - Gly180 N=7.4 Å). In the RMCP-I - ANG-I complex, contrastly, the 4-5 model could be preferable because the complex is highly stabilized by nine hydrogen bonds and the C-terminal moiety of ANG-I is tightly fixed by the electrostatic interaction with Lys27 side chain of RMCP-I; this is not the case in HC - ANG-I complex (Table I). Furthermore, the Thr29 side chain of RMCP-I, in contrast with the Phe29 in HC, allows the approach of Tyr4 - Ile5 amide bond of ANG-I to the active site *via* hydrogen bonds (Fig.3d).

Based on these findings, it could say that the 'up and down' undulation of electrostatic potentials around the active site of HC, especially Arg130 and Asp139, provides an important factor of determining its substrate-specificity against the ANG-I (ANG-II production); the Arg130 acts as the fixation of the C-terminal charge of ANG-I with the help of the interaction with Lys179 in

the 8-9 model, while the Asp139 keeps this charge away from the active site in the 4-5 model. On the other hand, in the case of RMCP-I, the stable complexes with ANG-I could be constructed in both the 8-9 and 4-5 models, and the binding diversity seems to be due to the abundant non-charged hydrophilic residues on the active site. However, it is noteworthy that the 4-5 cleavage model has the advantage in the number of hydrogen bonds and electrostatic interactions, compared with the 8-9 model.

In this modeling study, we predicted that the 27th, 29th, 130th, and 139th residues of chymases play important roles in recognizing the ANG-I molecule. These residues are all located at the binding site of substrate C-terminal moiety. This C-terminal binding site appears to be important to determine the substrate-specificity of chymase, judging from that (i) the positive charge of the 27th residue is closely related with the stability of the 4-5 cleavage model in ANG-I - RMCP-I complex and (ii) the positive charges of the 179th and 130th residues are related with the stability of the 8-9 cleavage model in the HC - ANG-I complex. The negative charge of Asp139 and the bulky side chain of Phe29 could disturb the 4-5 cleavage of ANG-I in the HC complex. The N-terminal moiety of ANG-I participates in electrostatic and hydrogen bonds with the polar atoms of HC in the 8-9 cleavage model.

In the biological event, intact chymase exhibits various functions [16], in addition to the production of ANG-II from ANG-I. Thus, the present models could not explain all biological aspects of the chymase. However, the *in vitro* enzymatic activities of HC and RMCP-I for ANG-I could be explained well by these models. In this context, the present results would provide useful information to consider the catalytic behavior of chymase at the molecular level and to design the species-specific inhibitors which can control the biological activity of chymase [17].

ACKNOWLEDGMENT

This work was supported in part by a Grant-in-Aid for Encouragement of Young Scientists No.08779976 to N. Shiota from the Ministry of Education, Science, Sports and Culture, Japan.

REFERENCES

1. Peart, W. S. (1978) *Johns. Hopkins. Med. J.* **143,** 193–206.
2. Becu-Villalobos, D., Lacau-Mengido, I. M., Thyssen, S. M., Diaz-Torga, G. S., and Libertun, C. (1994) *Am. J. Physiol.* **266,** E274–E278.
3. Okunishi, H., Miyazaki, M., and Toda, N. (1984) *J. Hypertens.* **2,** 277–284.
4. Okunishi, H., Miyazaki, M., Okamura, T., and Toda, N. (1987) *Biochem. Biophys. Res. Commun.* **149,** 1186–1192.
5. Okamura, T., Okunishi, H., Ayajiki, K., and Toda, N. (1990) *J. Cardiovasc. Pharmacol.* **15,** 353–359.
6. Okunishi, H., Oka, Y., Shiota, N., Kawamoto, T., Song, K., and Miyazaki, M. (1993) *Jpn. J. Pharmacol.* **62,** 207–210.
7. Shiota, N., Okinishi, H., Fukamizu, A., Sakonjo, H., Kikumori, M., Nishimura, T., Nakagawa, T., Murakami, K., and Miyazaki, M. (1993) *FEBS Lett.* **323,** 239–242.
8. Trong, H. L., Neurath, H., and Woodbury, R. G. (1987) *Proc. Natl. Acad. Sci. U.S.A.* **33,** 364–367.
9. Weiner, P., and Kollman, P. A. (1981) *J. Comput. Chem.* **2,** 287.
10. Brooks, B. R., Bruccoleri, R. E., Olafson, B. D., States, D. J., Swaminathan, S., and Karplus, M. J. (1983) *J. Comput. Chem.* **4,** 187–217.
11. Levitt, M. (1992) *J. Mol. Biol.* **226,** 507–533.
12. Elofsson, A., Kilinski, T., Rigler, R., and Nilsson, L. (1993) *Proteins,* **17,** 161–175.
13. Remington, S. J., Woodbury, R. G., Reynolds, R. A., Matthews, B. W., and Neurath, H. (1988) *Biochemistry,* **27,** 8097–8105.
14. Thompson, J. D., Higgins, D. G., and Gibson, T. J. (1994) *Nucl. Aci. Res.,* **22,** 4673–4680.
15. Jorgensen, W., Chandrasekar, J., Mandula, J., Impey, R., and Klein, M. (1983) *J. Chem. Phys.* **79,** 926–935.
16. Sali, A., Matsumoto, R., McNeil, H. P., Karplus, M., and Stevens, R. L. (1993) *J. Biol. Chem.* **268,** 9023–9034.
17. Niwata, S., Fukami, H., Sumida, M., Ito, A., Kakutani, S., Saitoh, M., Suzuki, K., Imoto, M., Shibata, H., Imajo, S., Kiso, Y., Tanaka, T., Nakazato, H., Ishihara, T., Takai, S., Yamamoto, D., Shiota, N., Miyazaki, M., Okunishi, H., Kinoshita, A., Urata, H., and Arakawa, K. (1997) *J. Med. Chem.* **40,** 2156–2163.
18. Henikoff, S., and Henikoff, J. G. (1992) *Proc. Natl. Acad. Sci. U.S.A* **89,** 10915–10919.
19. Vingron, M., and Waterman, M. S. (1993) *J. Mol. Biol.* **234,** 1–12.